

Supporting Information

A Selective Fluorescence Turn-on Sensing Coordination Polymer for Antibiotic Aztreonam

Xiaomei Wang,^a Cheng Liu,^a Ming Wang,^a Xinhui Zhou,^{*a} Yujian You^a and Hongping Xiao^{*b}

^a Key Laboratory for Organic Electronics and Information Displays & Jiangsu Key Laboratory for Biosensors, Institute of Advanced Materials, Jiangsu National Synergetic Innovation Center for Advanced Materials, Nanjing University of Posts & Telecommunications, Nanjing 210023, China. E-mail: iamxhzhou@njupt.edu.cn

^b College of Chemistry and Materials Engineering, Wenzhou University, Wenzhou 325035, China. E-mail: hp_xiao@126.com

EXPERIMENTAL SECTION

Materials and general methods

All chemicals used in this work are available commercially and were used without further purification.

Elemental analyses (C, H, N) were carried out on a Perkin-Elmer 240C analyzer. FT-IR spectra were measured in the range of 400-4000 cm⁻¹ with a PerkinElmer-Spectrum on KBr pellets. The thermogravimetric analysis (TGA) was performed from room temperature to 800 °C under a nitrogen atmosphere on a NETZSCH STA2500 simultaneous DTA-TG apparatus instrument. Powder X-ray diffraction patterns (PXRD) data of all samples were collected in the 5-50° range of 2θ with a scan step width of 0.02° on a Bruker D8 Advance A25 diffractometer (Cu-Kα, λ = 1.5418 Å). The UV-Vis absorption spectra were recorded on a LAMBDA 35 spectrophotometer. Photoluminescence spectra were carried out using a RF-5301PC spectrofluorophotometer at the room temperature. Fluorescence lifetimes of samples and the low temperature phosphorescence spectrum was measured using a Edinburgh

FLSP920 transient/stable fluorescence spectrometer. The low temperature fluorescence spectrum was measured using Hitachi F-4700.

Synthesis of complex 1

The mixture of H₄adip (25.3 mg, 0.05 mmol), Tb(NO₃)₃·6H₂O (37.3 mg, 0.1 mmol), terephthalic acid (8.4 mg, 0.05 mmol), H₂O (1 mL), NMP (2 mL), DMF (3 mL) was sealed in a 15 mL Teflon-lined stainless steel container. It was heated at 110 °C for 2 days and then slowly cooled to room temperature to obtain crystals of **1**. **1** was washed three times with DMF after removal of the mother liquid and finally dried in vacuum drying oven. Yield: 61% relatively to Tb. Elemental analysis calcd. for C₂₉H₂₇N₂O₈Tb(%): C, 50.45; N, 4.06; H, 3.94. Found: C, 50.36; N, 4.01; H, 3.91. IR (KBr, cm⁻¹): 3418 (w), 1611 (s), 1651 (s), 1549 (s), 1374 (s), 843 (m), 770 (m), 718 (m), 666 (m), 532 (w).

X-ray Crystal structure determination

Single-crystal X-ray diffraction data were collected on Bruker Smart Apex CCD diffractometer with graphite monochromated Mo-K α radiation ($\lambda = 0.71073 \text{ \AA}$) at 100(2) K and using the ω - θ scan mode in the ranges $1.867^\circ \leq \theta \leq 24.999^\circ$. Raw frame data were integrated with the SAINT program. The structures were solved by direct methods using SHELXS-2014¹ and refined by full-matrix least-squares on F² using SHELXL-2014.² An empirical absorption correction was applied with the program SADABS.³ All non-hydrogen atoms were refined anisotropically. All hydrogen atoms were positioned geometrically and refined as riding atoms. The crystallographic data and selected bond lengths and bond angles have been listed in Tables S1 and S2. The crystallographic data for the structural analysis have been deposited in the Cambridge Crystallographic Data Center with the CCDC reference number of 2131524.

Luminescence sensing experiment

A total of 1 mg of ground sample **1** was dispersed in 3 mL of DMF to prepare the **1**-DMF suspension. Then the **1**-DMF suspension was sonicated for 30 mins before each luminescence sensing experiment to make samples uniformly dispersed.

Calculation of the limit of detection

The limit of detection (LOD) was determined according to the definitions:

$$\sigma = \sqrt{\frac{\sum_{i=1}^n (x_i - \bar{x})^2}{n - 1}} \quad (1)$$

$$I/I_0 = K_{EC}[ATM] + b \quad (2)$$

$$LOD = 3\sigma/K_{EC} \quad (3)$$

Firstly, the standard deviation (σ) was calculated by measuring the fluorescence intensity of the blank solution for more than 10 times and then got the average intensity (\bar{x}). By fitting the data into equation (1), the value of standard deviation (σ) was obtained. Secondly, a certain amount of ATM was added into the 1-DMF and the resulting intensity (I) was recorded. By fitting the data into equation (2), where I_0 is the initial intensity without adding ATM, the value of precision K_{EC} was calculated. Finally, the limit of detection (LOD) was calculated according to equation (3).

Calculation details of LUMO and HOMO of H₄adip, H₂bdc and ATM

Density functional theory was used to optimize the geometry of the compounds at the B3LYP/def2-TZVP level. Vibrational frequency calculations were performed to verify the minimum nature of the optimized structures. The solvent effect of N, N-Dimethylformamide was considered by conductor-like polarizable continuum model (C-PCM),⁴ and the atom-pairwise dispersion correction with the Becke-Johnson damping scheme (D3BJ) was considered in the calculations.⁵⁻⁶ All above calculations were carried out by the ORCA program (5.0.1).⁷⁻⁸ The frontier molecular orbitals were analyzed on Multiwfn 3.8⁹ and VMD program.¹⁰

Table S1. Crystal data and structure refinement details for **1**.

Empirical formula	C ₂₉ H ₂₇ TbN ₂ O ₈	V/Å ³	1295.3(10)
Formula weight	690.44	Z	2
Temperature/K	100(2)	D_{calc} /(g·cm ⁻³)	1.770
Crystal system	Triclinic	μ /mm ⁻¹	2.787
Space group	$P\bar{1}$	$F(000)$	688
a/Å	9.397(4)	Reflections collected	9582

b/Å	10.471(5)	Unique reflections	5286
c/Å	15.004(7)	R_{int} , R_{sigma}	0.0294, 0.0438
α /°	73.416(10)	GOF (F^2)	1.371
β /°	78.485(10)	R_1^a , wR_2^b ($I > 2\sigma(I)$)	0.0446, 0.1520
γ /°	66.927(9)	R_1^a , wR_2^b (all data)	0.0453, 0.1533

$$R_1^a = \sum ||F_o| - |F_c|| / \sum |F_o|. \quad wR_2^b = [\sum w(F_o^2 - F_c^2)^2 / \sum w(F_o^2)]^{1/2}.$$

Table S2. Selected bond lengths (Å) for **1**.

Tb(1)-O(1)	2.335(4)	Tb(1)-O(2) ^{#1}	2.288(4)
Tb(1)-O(3) ^{#2}	2.406(4)	Tb(1)-O(4) ^{#2}	2.469(4)
Tb(1)-O(5)	2.386(5)	Tb(1)-O(6)	2.460(4)
Tb(1)-O(7)	2.331(4)	Tb(1)-O(8)	2.356(4)
O(1)-Tb(1)-O(3) ^{#2}	79.42(14)	O(8)-Tb(1)-O(3) ^{#2}	79.50(15)
O(7)-Tb(1)-O(6)	76.49(17)	O(5)-Tb(1)-O(3) ^{#2}	104.13(18)
O(1)-Tb(1)-O(5)	151.44(15)	O(2) ^{#1} -Tb(1)-O(6)	77.96(14)
O(8)-Tb(1)-O(5)	74.51(16)	O(1)-Tb(1)-O(6)	146.73(12)
O(2) ^{#1} -Tb(1)-O(3) ^{#2}	158.44(15)	O(8)-Tb(1)-O(6)	125.93(14)
O(7)-Tb(1)-O(3) ^{#2}	93.9(2)	O(5)-Tb(1)-O(6)	53.57(16)
O(2) ^{#1} -Tb(1)-O(7)	94.2(2)	O(3) ^{#2} -Tb(1)-O(6)	123.42(13)
O(2) ^{#1} -Tb(1)-O(1)	82.72(13)	O(2) ^{#1} -Tb(1)-O(4) ^{#2}	148.49(15)
O(7)-Tb(1)-O(1)	78.23(16)	O(7)-Tb(1)-O(4) ^{#2}	77.0(2)
O(2) ^{#1} -Tb(1)-O(8)	85.18(16)	O(1)-Tb(1)-O(4) ^{#2}	123.68(17)
O(7)-Tb(1)-O(8)	156.5(2)	O(8)-Tb(1)-O(4) ^{#2}	114.7(2)
O(1)-Tb(1)-O(8)	78.42(14)	O(5)-Tb(1)-O(4) ^{#2}	76.9(2)
O(2) ^{#1} -Tb(1)-O(5)	86.07(18)	O(3) ^{#2} -Tb(1)-O(4) ^{#2}	53.05(14)
O(7)-Tb(1)-O(5)	128.91(18)	O(6)-Tb(1)-O(4) ^{#2}	70.58(14)

Symmetry codes: ^{#1}1-x, 1-y, 2-z; ^{#2}-x, 2-y, 2-z.

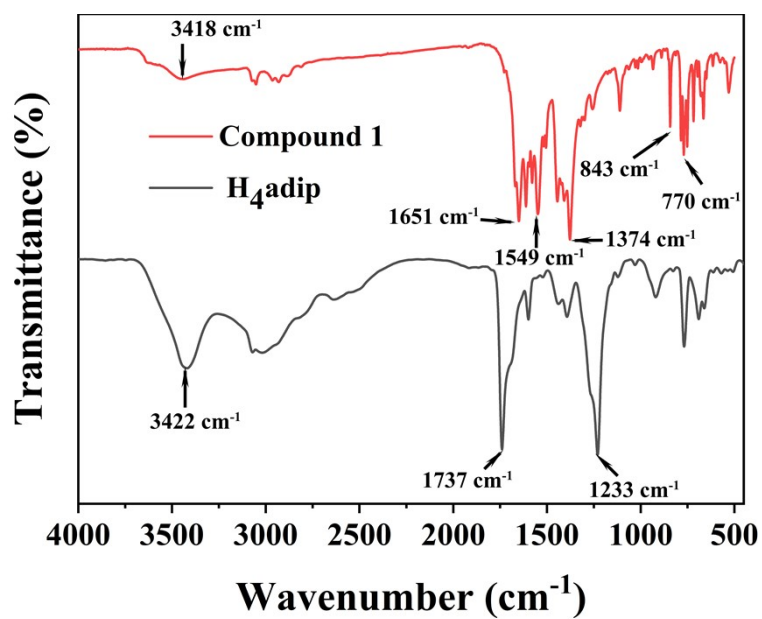


Figure S1. IR spectra of **1**.

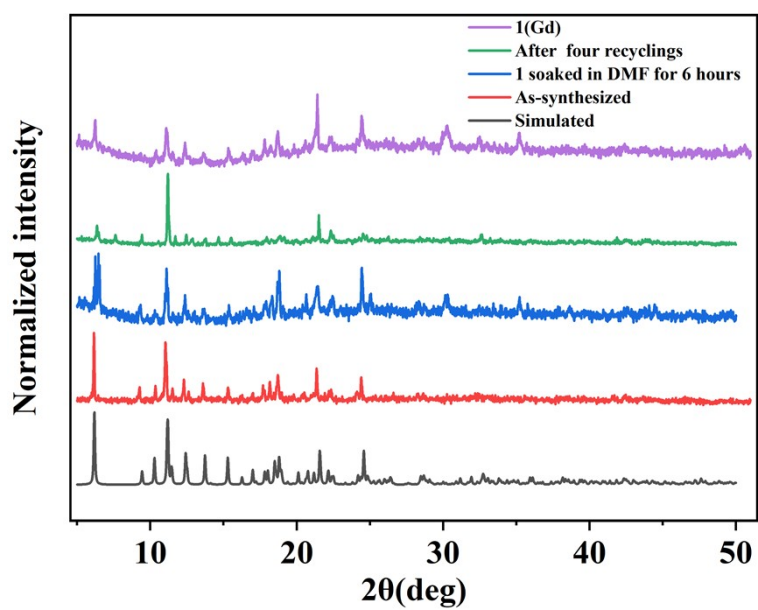


Figure S2. The PXRD patterns of **1** and **1(Gd)**.

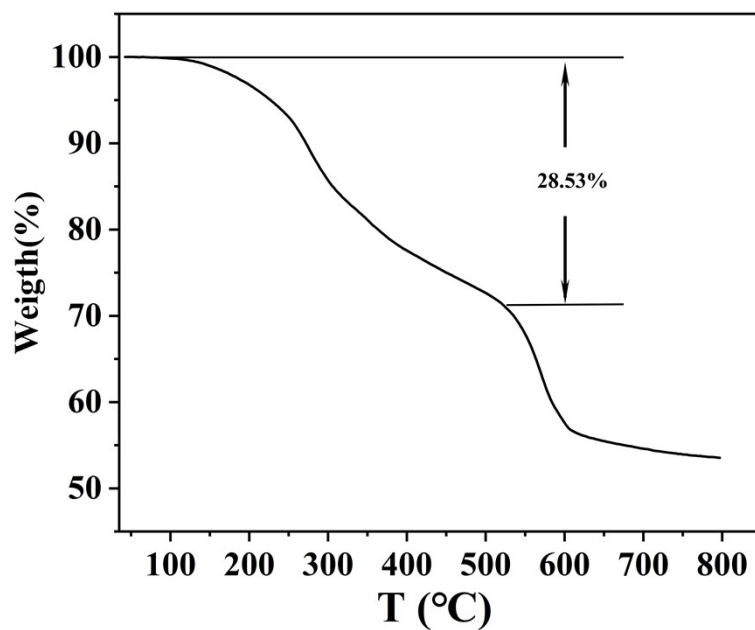


Figure S3. Thermogravimetric curve of the 1.

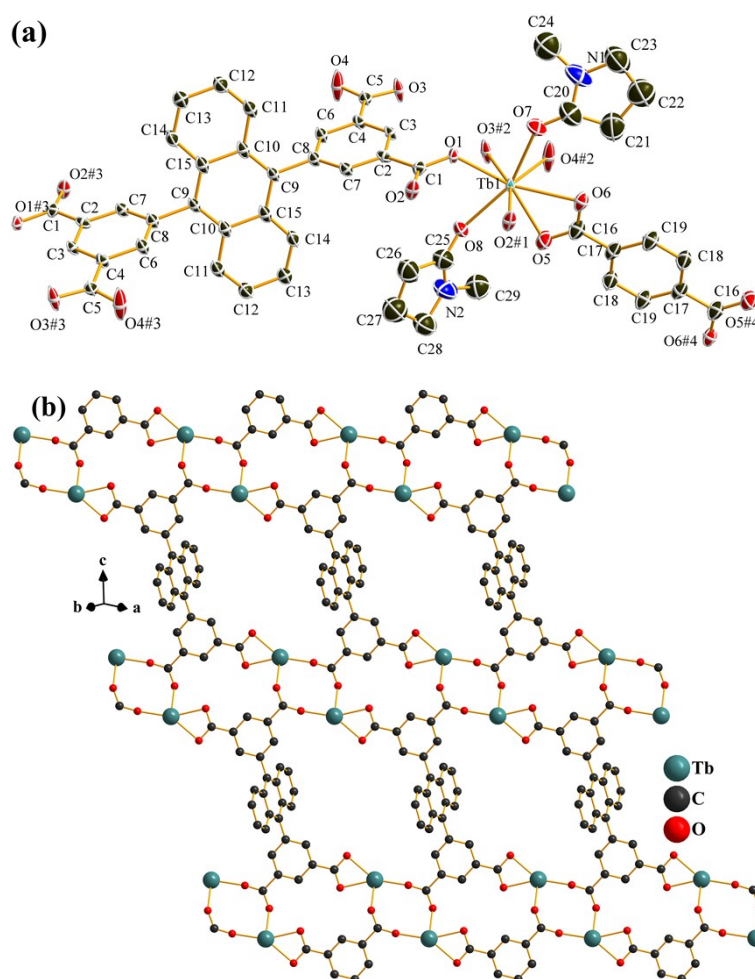


Figure S4. (a) The asymmetric unit of 1 with the thermal ellipsoids drawn at the 50% probability level. (b) The 2D coordination network lying on (111) crystal plane. All

hydrogen atoms in (a), (b), and NMP molecules in (b), are omitted for clarity.

Symmetry codes: #1 1-x, 1-y, 2-z; #2 -x, 2-y, 2-z; #3 1-x, 2-y, 1-z; #4 1-x, 1-y, 3-z.

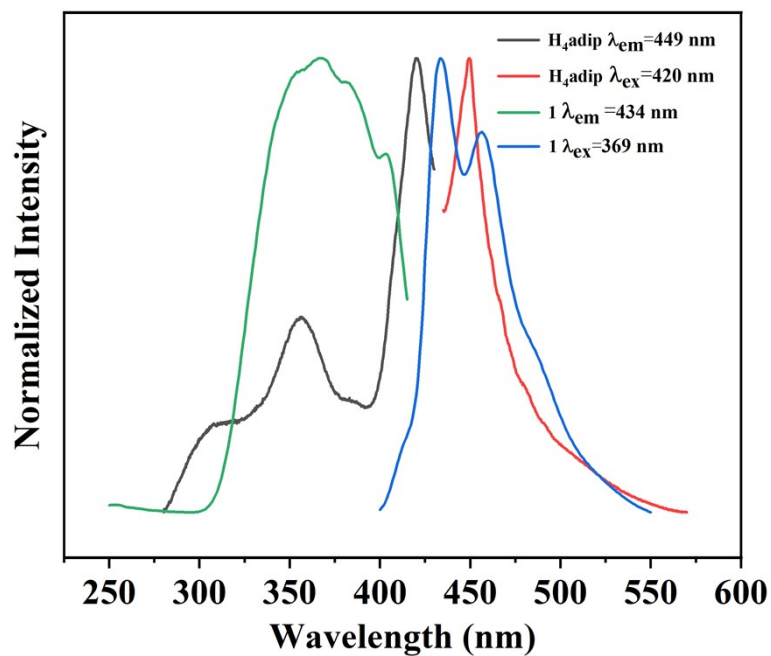


Figure S5. Solid-state luminescent spectra of H₄adip and 1.

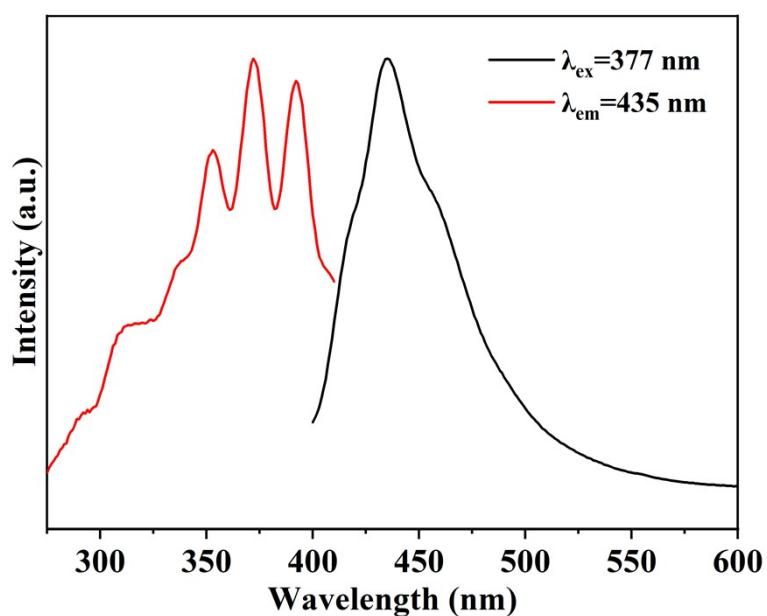


Figure S6. Excitation and emission spectra of 1-DMF suspension.

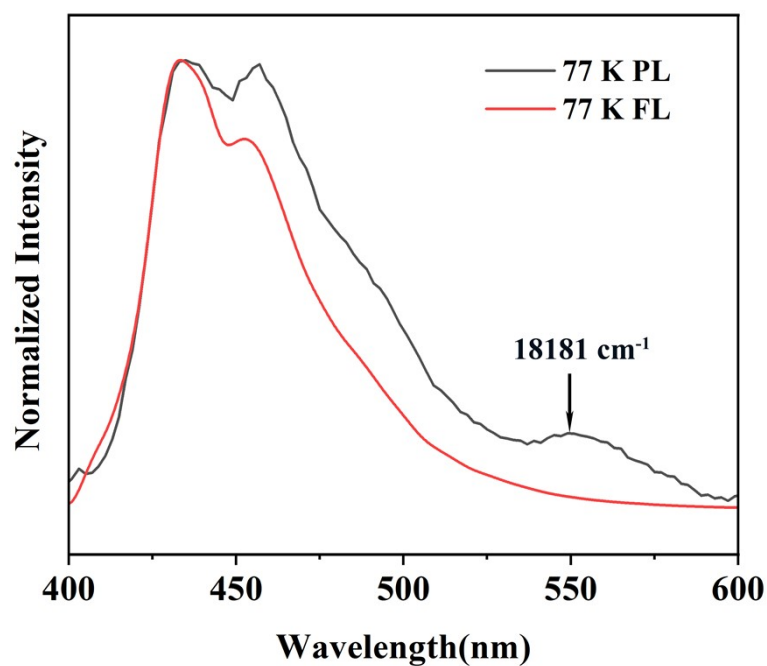


Figure S7. Fluorescence and phosphorescence spectra of **1(Gd)** at 77 K (excited at 369 nm).

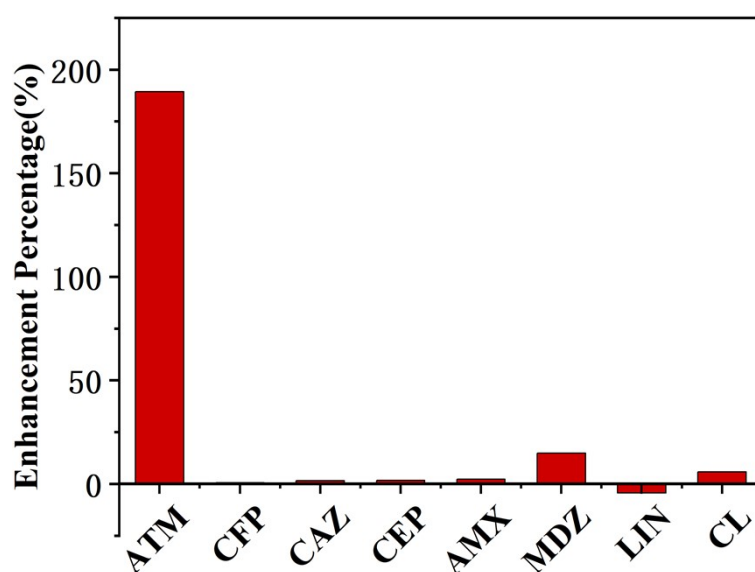


Figure S8. Upon excitation at 377 nm, the fluorescence enhancement percentages of **1-DMF** suspension for intensities of emission peak at 435 nm after the addition of different kinds of antibiotics (0.1 mM).

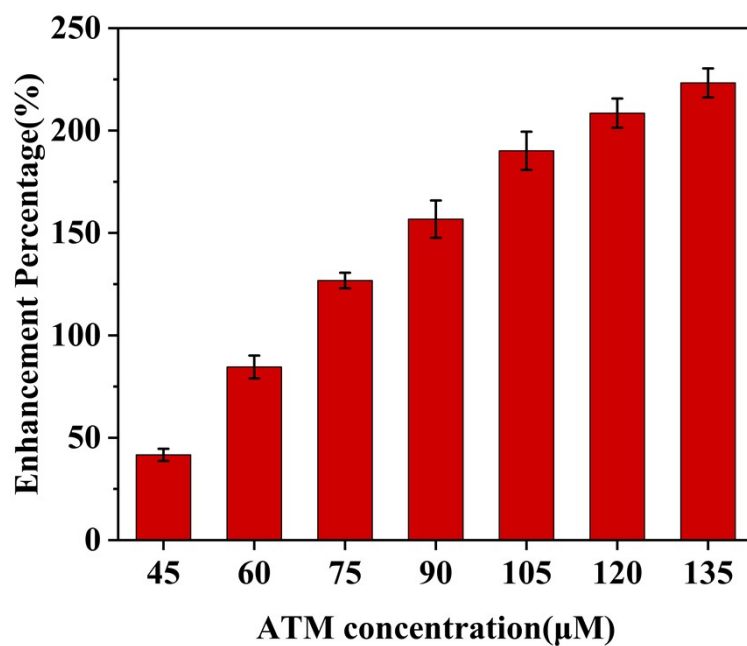


Figure S9. The fluorescence enhancement percentages after adding different concentrations of ATM.

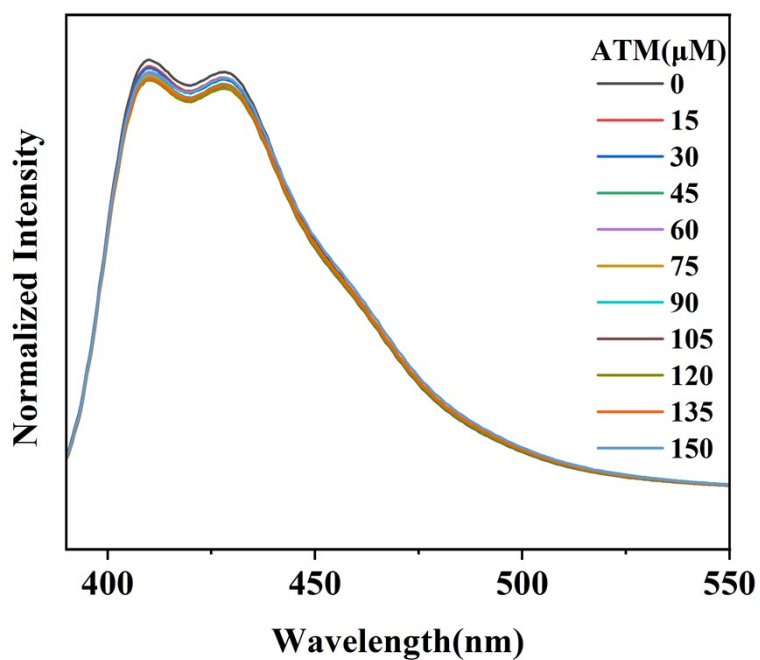


Figure S10. The emission spectra (excited at 375nm) of H_2bdc in DMF after adding different concentrations of ATM.

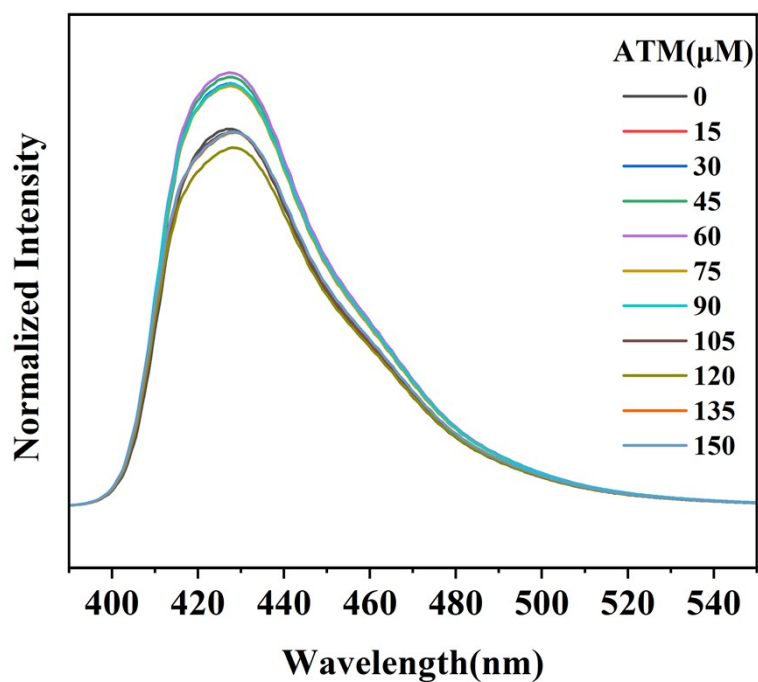


Figure S11. The emission spectra (excited at 377nm) of H₄adip in DMF after adding different concentrations of ATM.

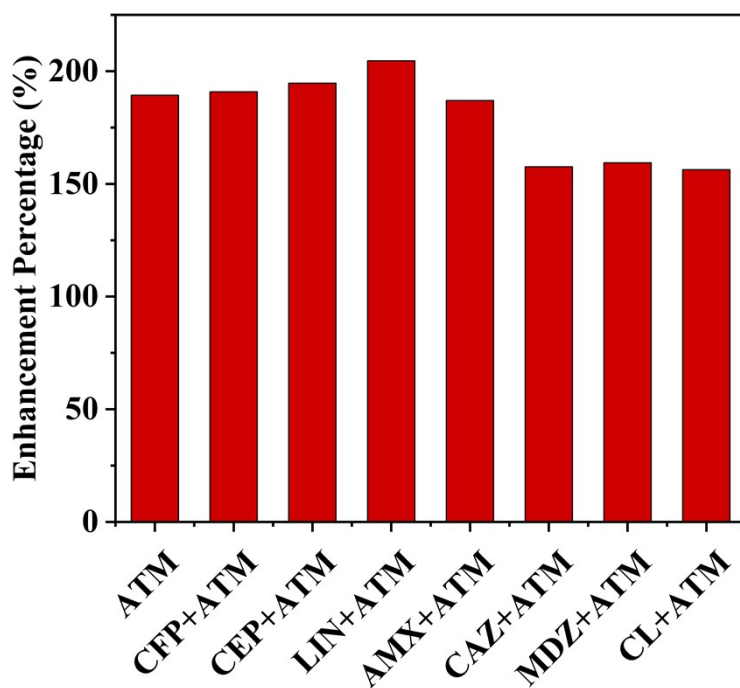


Figure S12. The fluorescence enhancement percentages when 1-DMF suspension was treated with ATM (0.1 mM) and other interfering antibiotics (0.1 mM).

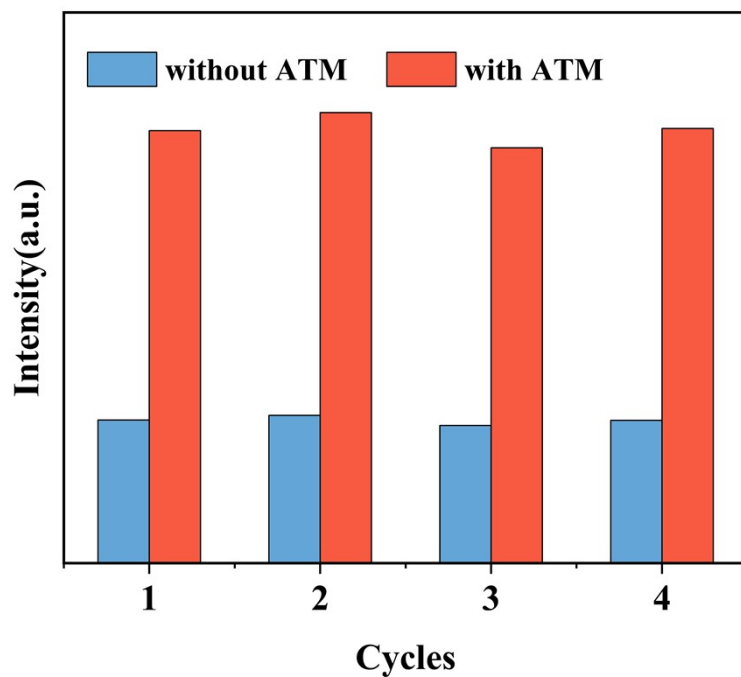


Figure S13. Four cycles test of 1-DMF suspension for ATM (0.1 mM).

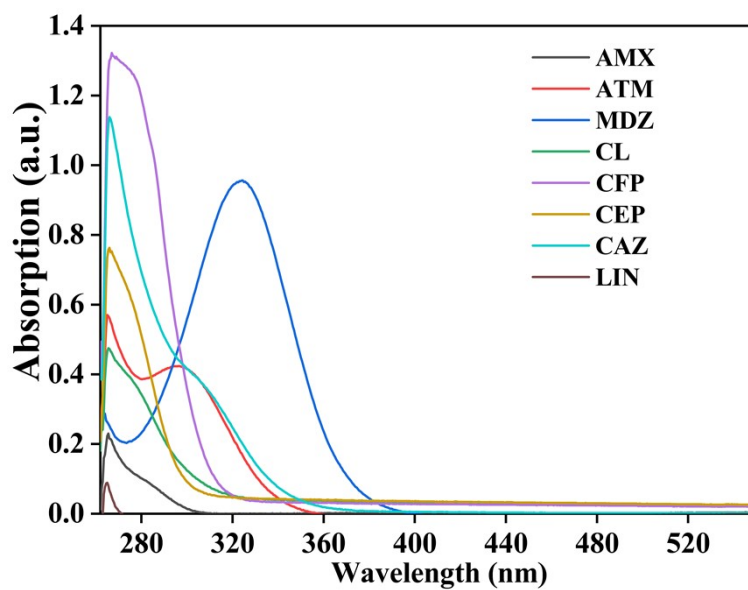


Figure S14. UV-Vis absorption spectra of the antibiotics in DMF.

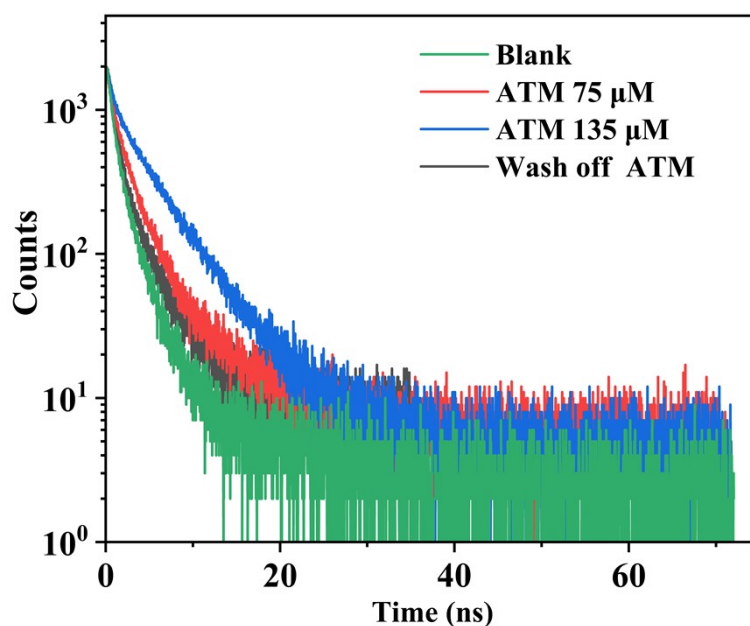


Figure S15. Fluorescence lifetime spectra of **1**.

References

- 1 G. M. Sheldrick, SHELXS-2014, Program for Crystal Structure Solution, University of Gottingen, Germany, 2014.
- 2 G. M. Sheldrick, SHELXL-2014, Program for the Refinement of Crystal Structure, University of Gottingen, Germany, 2014.
- 3 G. M. Sheldrick, SADABS, Program for Empirical Absorption Correction of Area Detector Data, University of Gottingen, Gottingen Germany, 1997.
- 4 V. Barone and M. Cossi, *J. Phys. Chem. A.*, 1998, **102**, 1995.
- 5 S. Grimme, S. Ehrlich and L. Goerigk, *J. Comput. Chem.*, 2011, **32**, 1456.
- 6 S. Grimme, J. Antony, S. Ehrlich and H. Krieg, *J. Chem. Phys.*, 2010, **132**, 154104.
- 7 F. Neese, *WIREs Comput. Mol. Sci.*, 2012, **2**, 73.
- 8 F. Neese, *WIREs Comput. Mol. Sci.*, 2018, **8**, e1327.
- 9 T. Lu and F. Chen, *J. Comput. Chem.*, 2012, **33**, 580.
- 10 W. Humphrey, A. Dalke and K. Schulten, *J. Molec. Graphics*, 1996, **14**, 33.